ChemPubSoc Europe

DOI: 10.1002/cphc.201201061

Supramolecular Cl···H and O···H Interactions in Self-Assembled 1,5-Dichloroanthraquinone Layers on Au(111)

Seung-Kyun Noh,[a] Jeong Heum Jeon,[a] Won Jun Jang,[a] Howon Kim,[a] Soon-Hyeong Lee,[a] Min Wook Lee,[a] Jhinhwan Lee,*[b] Seungwu Han,[c] and Se-Jong Kahng*[a]

The role of halogen bonds in self-assembled networks for systems with Br and I ligands has recently been studied with scanning tunneling microscopy (STM), which provides physical insight at the atomic scale. Here, we study the supramolecular interactions of 1,5-dichloroanthraquinone molecules on Au(111), including Cl ligands, by using STM. Two different molecular structures of chevron and square networks are observed, and their molecular models are proposed. Both molecular structures are stabilized by intermolecular Cl···H and O···H hydrogen bonds with marginal contributions from Cl-related halogen bonds, as revealed by density functional theory calculations. Our study shows that, in contrast to Br- and I-related halogen bonds, Cl-related halogen bonds weakly contribute to the molecular structure due to a modest positive potential (σ hole) of the Cl ligands.

1. Introduction

Covalently bonded halogen atoms (X) have unusual charge distributions, possessing both positive and negative potential regions.[1–5] The negative region acts as electron donor to form X···H hydrogen bonds. The positive region, termed σ hole, acts as electron acceptor to form X···O halogen bonds. Between two halogen ligands, X···X halogen bonds also form. Halogen bonds compete with hydrogen bonds in making supramolecular structures of functional biomolecules.[6–13] Halogen bonds and hydrogen bonds are similar in bond strengths and dissimilar in directionality. Halogen bonds have been found in various drug candidates, for which halogen ligands are widely used to enhance membrane permeability.[14–16] Recent studies showed that halogen bonds can be used to form supramolecular networks with possible applications in nanotechnology, and detailed structures of molecular networks have been characterized using scanning tunneling microscopy (STM) on metal surfaces.[17–22] For example, it has been reported that well-ordered two-dimensional (2D) networks of 1,5-dibromoanthraquinones (DBAQ) molecules are formed due to the contribution of intermolecular Br···Br, Br···H, and O···H bonds on Au(111).[18] STM studies on halogen-related bonds have been performed only for Br-and I-halogen ligands, but not for Cl ligands.

The strength of the σ hole is dependent on the overall size of the valence electron orbitals of the halogen atom.[2–4] The larger the effective radius of the valence electrons is, the stronger is the σ-hole strength. Therefore, the σ-hole of a Cl ligand is weaker than that of a Br ligand. However, recent reports have shown that Cl···Cl halogen bonds are formed in molecules such as hexachlorobenzene, 2-chloro-3-chloromethyl-8-methylquinoline, and 3,4,5-trichloropyridine.[23–25] On the basis of X-ray crystallography analyses, these reports demonstrated that Cl ligands are reasonable donors and acceptors for halogen bonds in the bulk crystals of these molecules

Our goal was to inspect if similar halogen bonds form on surfaces using STM. In this paper, we report on the intermolecular interactions of 1,5-dichloroanthraquinones (DCAQ) molecules on Au(111), in comparison with DBAQ. DCAQ forms two different molecular structures by means of Cl···H and O···H hydrogen bonds. The contribution of Cl···Cl halogen bonds is modest in this system.

2. Results and Discussion

An atomic model of the DCAQ molecule is shown in Figure 1a. The electrostatic potential was calculated using DFT methods based on the generalized gradient approximation (GGA) and mapped on isosurfaces of 0.003 e Bohr^{-3}. H and O atoms show positive and negative electrostatic potentials, reflecting their difference in electronegativity (2.55 and 3.04). The σ hole of the Cl atoms is depicted as white region embedded in a black region of cylindrical symmetry around the axis of the covalent

[a] S.-K. Noh, J. H. Jeon, W. J. Jang, Dr. H. Kim, S.-H. Lee, M. W. Lee, Prof. S.-J. Kahng
Department of Physics, Korea University
1-5 Anam-dong, Seongbuk-gu
Seoul, 136-713 (Republic of Korea)
E-mail: sjkahng@korea.ac.kr

[b] Prof. J. Lee
Department of Physics, KAIST
Daejeon, 305-701 (Republic of Korea)
E-mail: jhinhwan@kaist.ac.kr

[c] Prof. S. Han
Department of Materials Science and Engineering
Seoul National University
Seoul 151-744 (Republic of Korea)

Supporting information for this article is available on the WWW under http://dx.doi.org/10.1002/cphc.201201061.

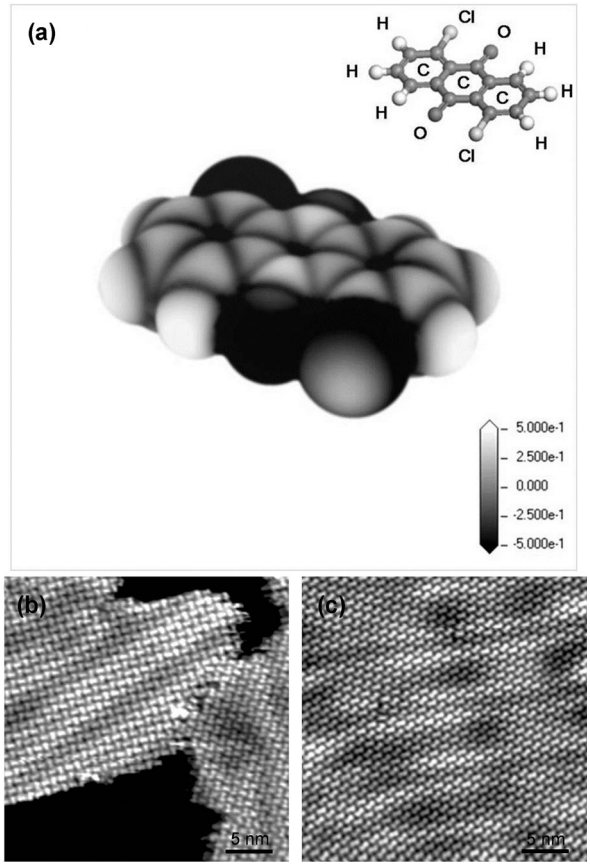

Figure 1. a) Molecular structures and calculated molecular electrostatic potential distributions (in Volt) of DCAQ molecules at isodensity surfaces, shown in white (positive) and black (negative).14 carbon atoms form three hexagons which are terminated with 6 H, 2 O, and 2 Cl atoms. b) and c) Typical STM images, measured at 80 K, of the 2D supramolecular structures of DCAQ molecules as-deposited at about 150 K. The square (b) and chevron (c) structure are visible. Size of both STM images: 30×30 nm^2.Tunneling current: $I_T=0.1$ nA. Sample voltage: $V_S=-1.8$ V.

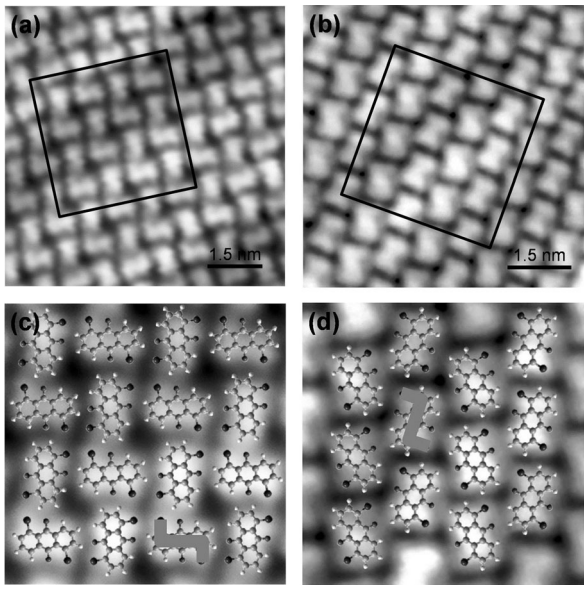

Figure 2. Higher resolution (compared to Figure 1) STM images of the a) square and the b) chevron structure. Magnified STM regions of (a) and (b) of the c) square and the d) chevron structures superimposed by the molecular models. Individual molecules can be identified by their z-shapes in grey. Sizes of the STM images: (a) and (b) 7.5×7.5 nm^2, (c) and (d) 4×4 nm^2. Tunneling current: $I_T=0.1$ nA. Sample voltage: $V_S=-1.8$ V.

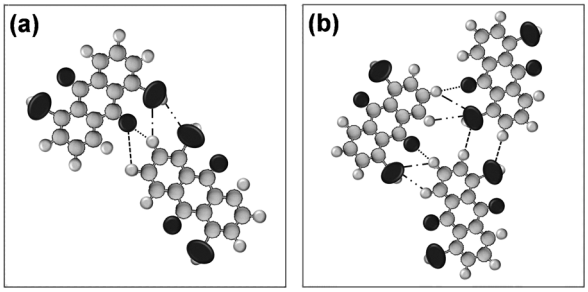

Figure 3. Illustrations of the possible interactions between a) two nearest neighbor and b) three nearest neighbor DCAQ molecules with simplified electrostatic potential distributions around their H, O, and Cl atoms. a) Dashed lines and dotted lines: O···H bonds; dash-dotted lines and dash-double-dotted lines: Cl···H and Cl···Cl bonds b) Dotted lines: O···H bonds; all other lines: Cl···H bonds.

bond. Note that the size of the σ hole of a Cl atom is small compared with that of a Br atom (see the Supporting Information). The DCAQ molecules deposited on Au(111) form molecular islands at 150 K. Figure 1 b shows a typical STM image obtained after about 0.8 monolayers of DCAQ were deposited on the substrate. We observed a one monolayer-high molecular layer that preserved the herringbone corrugations of Au(111) at 80 K. The molecular layer was made of two different network structures, square and chevron, as shown in Figure 1 b, c.

Small-scale images of the two structures are shown in Figure 2. Individual molecules can be identified by their z-shape. The STM images in Figure 2 c, d are superimposed by the molecular models. To identify the intermolecular interactions in the two structures, the structures of two and three neighboring molecules are drawn in Figure 3 a, b, along with simplified versions of the electrostatic potential distributions around Cl, O, and H, based on the single molecule potential shown in Figure 1 a. In the square structure, two neighboring DCAQ molecules can have four possible intermolecular bonds. The dashed and dotted lines denote two O···H bonds, while the dash-dotted and dash-double-dotted lines show a Cl···H and a Cl···Cl bond. In the chevron structure, three neighboring DCAQ molecules have eight possible intermolecular bonds that are classified into four different kinds of bonds, an O···H bond (dotted lines) and three Cl···H bonds (dashed lines, dash-dotted lines, and dash-double-dotted lines).

DFT calculations were performed to understand the precise arrangement of the DCAQ molecules in the square and chevron structures. The results, shown in Figure 4 a, b, clearly reproduce our models in Figure 2. In the square structure, the long axes of two neighboring DCAQ molecules are at an angle of 90°, and the equilibrium lattice distances (the magnitude of the unit-cell vectors) are 1.34 nm, which is consistent with experimental observations (89° and 1.3 nm). In the chevron structure, the long axes of two neighboring DCAQ molecules across two parallel rows of molecules are at an angle of 58.5°. The

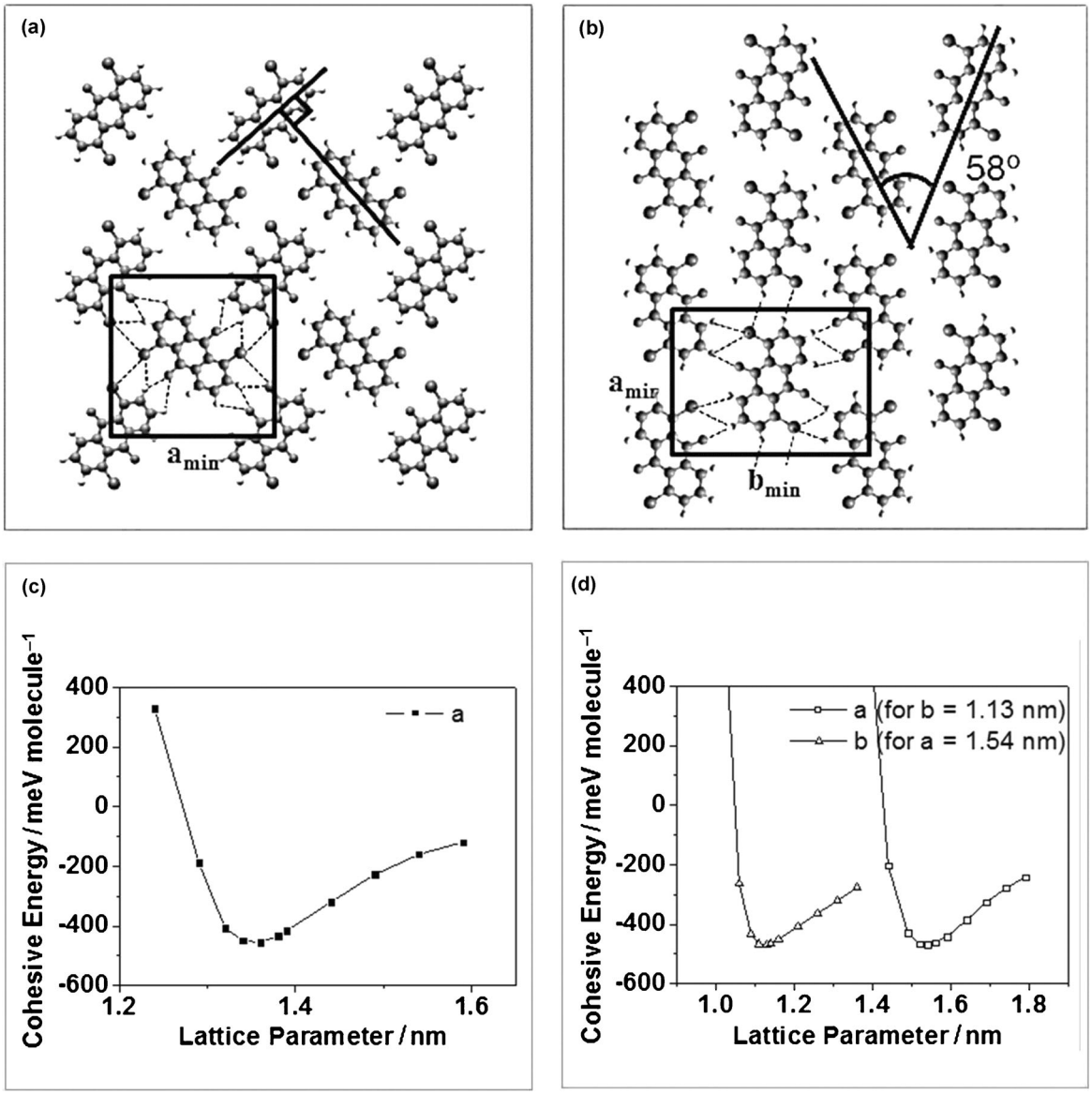

Figure 4. Relaxed a) square and b) chevron structures of DCAQ obtained from DFT calculations. The square and a rectangle show unit cells in (a) and (b) with unit vectors. 16 possible intermolecular interactions are drawn with dotted lines for a molecule in the unit cells in (a) and (b). Energy gains per molecule as a function of lattice parameters for the c) square and the d) chevron structure. Circles, triangles and squares are results of the calculations, curves represent fittings. For the chevron structure, only two graphs are selected for display. For the sake of simplicity the angle and the ratio between a and b were fixed, during the calculations, however, we considered them as independent variables.

equilibrium lattice distances along two orthogonal directions were 1.54 and 1.13 nm. They show reasonable agreement with experimental observations (58°, 1.5 and 1.1 nm). Since the calculations reproduce the model in Figure 2 well, they are used to extract the lengths of the possible intermolecular bonds considered in Figure 1. The results are summarized in Figure 5 (and listed in Table S1). The sum of the van der Waals radii for each bond are also drawn with dotted lines. In the square structure, the distances of the O···H (dotted lines) and the Cl···H (dash-dotted lines) bonds are smaller than the sum of the van der Waals radii. In the chevron structure, the distances of the O···H (dotted lines) and the two Cl···H (dashed lines and dash-double-dotted lines) bonds are smaller than or equal to the

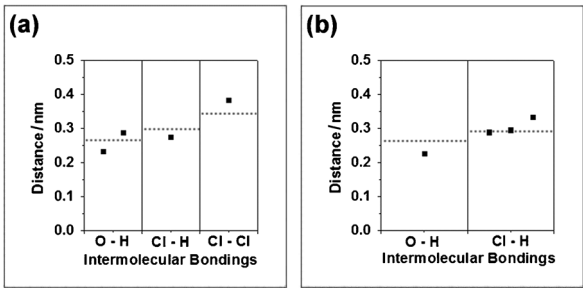

Figure 5. Measured distances for possible intermolecular bonds are represented with filled square marks in the a) square and the b) chevron structures, and their sums of the van der Waals radii are drawn with dotted lines as reference.

sum of the van der Waals radii. Therefore, both structures are strongly dependent on the O···H and the Cl···H bonds. The O···H bonds are short (0.23 nm) compared with the sum of the van der Waals radii (0.27 nm). Because the O···H bonds are so strong, the role of the halogen bond tends to be marginal; the chevron structure does not have any Cl···Cl bond, and the square structure has only a very weak Cl···Cl interaction whose distance is 0.38 nm, which larger than the sum of the van der Waals radii (0.35 nm).The distance of the Cl···H bond, denoted with dash-double-dotted lines in the chevron structure, is shorter than the sum of the van der Waals radii, even though the H atom faces both the positive and the negative potential regions of the Cl atom. This Cl···H bond seems to be stabilized by the help of the other two Cl···H bonds, denoted with dashed lines and dash-dotted lines in Figure 4b.

The binding energies obtained from the DFT calculations using GGA with van der Waals interactions were 455 and 469 meV per molecule for the square and the chevron structure, as shown in Figure 1c,d. In order to correctly compare binding energies, calculations including the substrate lattices should be made. We only performed gas-phase calculations to avoid shear calculation costs. We observed that the square and the chevron networks coexist in samples prepared at 150 K, and the chevron network occupies about 70% of the network area. When these samples were warmed up to 300 K and subsequently cooled down, only the chevron structure could be observed.[19,31] The square structure underwent a phase transformation during the heating and cooling processes, implying that the chevron structure is more stable than the sqaure structure. Thus, the two polymorphs at low temperature originate from kinetic limitation in molecular diffusion at 150 K. At elevated temperatures of 300 K, the molecules have a high enough kinetic energy to construct a stable chevron structure at the expense of the square structure.

3. Conclusions

Intermolecular interactions were studied in the self-assembled layers of DCAQ on Au(111) using scanning tunneling microscopy. Two kinds of molecular structures, chevron and square networks were observed, and their molecular models were explained on the bases of DFT calculations. Both molecular structures were stabilized by intermolecular O···H and Cl···H hydrogen bonds. Our study shows that Cl-related halogen bonds weakly contribute to the molecular structures due to the modest positive potential of the Cl-ligands, calling for further study regarding Cl-related halogen bonds.

Experimental Methods

STM experiments were performed using a home-built STM housed in an ultra-high vacuum chamber with a base pressure below 7×10^{-11} torr. The Au(111) surface was prepared from a thin film (200 nm thick) of Au on mica that was exposed to several cycles of Ne-ion sputtering and annealing at 800 K over the course of 1 h. The cleanliness of the Au(111) surface was checked by STM, and the typical herringbone structures were observed. Commercially available 1,5-DCAQ (Tokyo Chemical Industry) was outgassed in vacuum for several hours and then deposited on the Au(111) surface at submonolayer coverage by thermal evaporation using an alumina-coated evaporator. STM images were obtained at constant-current mode with a Pt/Rh tip while keeping the sample temperature at 80 K.

Theoretical Calculations

We performed ab initio density functional calculations (DFT) using the VASP code.[25,26] Interactions between ions and electrons were approximated by the projector-augmented wave (PAW) potential.[28] The generalized gradient approximation (GGA) with the Perdew–Burke–Ernzerhof (PBE) functional was used to describe the exchange correlations between electrons.[29] The energy cut-off for the plane wave basis was set to 600 eV. To describe non-bonding interactions between the molecules, in particular the van der Waals type, an empirical correction scheme proposed by Grimme et al. was adopted.[30] The energy and electrostatic potentials for the isolated molecules were obtained using a $35\times35\times20$ Å^3 supercell. A simulation cells containing two DCAQ molecules was adopted to describe the periodic structure, as depicted along with unit vectors in Figure 4a,b. The height of the simulation box perpendicular to the molecule plane was fixed at 10 Å, and the lateral cell parameters were optimized such that the residual stress was reduced to under 1 kbar.

Acknowledgements

The authors gratefully acknowledge financial support from National Research Foundation of Korea, and from the Ministry of Education Science and Technology of the Korean government (2010-0025301 and 2012-0013222). S.H. was supported by the Quantum Metamaterials Research Center (R11-2008-053-03001-0). This study was supported by the Supercomputing Center/Korea Institute of Science and Technology Information with supercomputing resources including technical support (KSC-2012-C1-10).

Keywords: halogen bonds · hydrogen bonds · molecular nanostructures · scanning tunneling microscopy · self-assembly

[1] O. Hassel, *Science* **1970**, *170*, 497.
[2] P. Metrangolo, G. Resnati, H. D. Arman, *Halogen Bonding: Fundamental and Applications*, Springer, Berlin, **2008**.
[3] G. R. Desiraju, R. Parthasarathy, *J. Am. Chem. Soc.* **1989**, *111*, 8725.
[4] P. Metrangolo, F. Meyer, T. Pilati, G. Resnati, G. Terraneo, *Angew. Chem.* **2008**, *120*, 6206; *Angew. Chem. Int. Ed.* **2008**, *47*, 6114.
[5] P. Metrangolo, G. Resnati, *Science* **2008**, *321*, 918.
[6] R. Paulini, K. Müller, F. Diederich, *Angew. Chem.* **2005**, *117*, 1820; *Angew. Chem. Int. Ed.* **2005**, *44*, 1788.
[7] O. Navon, J. Bernstein, V. Khodorkovsky, *Angew. Chem.* **1997**, *109*, 640; *Angew. Chem. Int. Ed. Engl.* **1997**, *36*, 601.
[8] H. F. Lieberman, R. J. Davey, D. M. T. Newsham, *Chem. Mater.* **2000**, *12*, 490.
[9] C. L. D. Gibb, E. D. Stevens, B. C. Gibb, *J. Am. Chem. Soc.* **2001**, *123*, 5849.
[10] E. Corradi, S. V. Meille, M. T. Messina, P. Metrangolo, G. Resnati, *Angew. Chem.* **2000**, *112*, 1852; *Angew. Chem. Int. Ed.* **2000**, *39*, 1782.
[11] C. B. Aakeröy, M. Fasulo, N. Schultheiss, J. Desper, C. Moore, *J. Am. Chem. Soc.* **2007**, *129*, 13772.

[12] C. Estarellas, A. Frontera, D. Quiñonero, P. M. Deyà, *ChemPhysChem* **2011**, *12*, 2742.
[13] A. Forni, S. Pieraccini, S. Rendine, F. Gabas, M. Sironi, *ChemPhysChem* **2011**, *13*, 4224 – 4234.
[14] M. Z. Hernandes, S. M. T. Cavalcanti, D. R. M. Moreira, W. F. de Azevedo, A. C. L. Leite, *Curr. Drug Targets* **2010**, *11*, 303 – 314.
[15] A. C. L. Leite, D. R. M. Moreira, M. V. O. Cardoso, M. Z. Hernandes, V. R. A. Pereira, R. O. Silva, A. C. Kiperstok, M. S. Lima, M. B. P. Soares, *ChemMedChem* **2007**, *2*, 1339.
[16] G. Gerebtzoff, X. Li-Blatter, X. H. Fischer, A. Frentzel, A. Seelig, *ChemBioChem* **2004**, *5*, 676.
[17] H. Walch, R. Gutzler, T. Sirtl, G. Eder, M. Lackinger, *J. Phys. Chem. C* **2010**, *114*, 12604.
[18] J. K. Yoon, W. J. Son, K. H. Chung, H. Kim, S. Han, S. J. Kahng, *J. Phys. Chem. C* **2011**, *115*, 2297.
[19] J. K. Yoon, W. J. Son, H. Kim, K. H. Chung, S. Han, S. J. Kahng, *Nanotechnology* **2011**, *22*, 275705.
[20] J. C. Russell, M. O. Blunt, J. M. Garfitt, D. J. Scurr, M. Alexander, N. R. Champness, P. H. Beton, *J. Am. Chem. Soc.* **2011**, *133*, 4220.
[21] R. Gutzler, O. Ivasenko, Ch. Fu, J. L. Brusso, F. Rosei, D. F. Perepichka, *Chem. Commun.* **2011**, *47*, 9453.
[22] K. H. Chung, J. Park, K. Y. Kim, J. K. Yoon, H. Kim, S. Han, S. J. Kahng, *Chem. Commun.* **2011**, *47*, 11492.
[23] T. T. T. Bui, S. Dahaoui, C. Lecomte, G. R. Desiraju, E. Espinosa, *Angew. Chem.* **2009**, *121*, 3896 – 3899; *Angew. Chem. Int. Ed.* **2009**, *48*, 3838 – 3841.
[24] V. R. Hathwar, T. N. Guru Row, *J. Phys. Chem. A* **2010**, *114*, 13434 – 13441.
[25] R. Wang, T. S. Dols, C. W. Lehmann, U. Englert, *Chem. Commun.* **2012**, *48*, 6830 – 6832.
[26] G. Kresse, J. Hafner, *Phys. Rev. B* **1993**, *47*, 558.
[27] G. Kresse, J. Hafner, *Phys. Rev. B* **1994**, *49*, 14251.
[28] P. E. Blöchl, *Phys. Rev. B* **1994**, *50*, 17953.
[29] J. P. Perdew, K. Burke, M. Ernzerhof, *Phys. Rev. Lett.* **1996**, *77*, 3865.
[30] S. Grimme, *J. Comput. Chem.* **2004**, *25*, 1463.
[31] P. A. Staniec, L. M. A. Perdigão, A. Saywell, N. R. Champness, P. H. Beton, *ChemPhysChem* **2007**, *8*, 2177.

Received: December 18, 2012
Published online on March 4, 2013